

# Seismic collapse safety of high-rise RC moment frames supported on two ground levels

Yun-Tian Wu<sup>\*1</sup>, Qing Zhou<sup>2</sup>, Bin Wang<sup>2</sup>, Yeong-Bin Yang<sup>2</sup> and Tian-Qing Lan<sup>2</sup>

<sup>1</sup>Key Laboratory of New Technology for Construction of Cities in Mountain Area, Ministry of Education; School of Civil Engineering, Chongqing University, Chongqing 400045, China

<sup>2</sup>School of Civil Engineering, Chongqing University, Chongqing 400045, China

(Received April 24, 2017, Revised February 27, 2018, Accepted March 7, 2018)

**Abstract.** Reinforced concrete (RC) moment frames supported on two ground levels have been widely constructed in mountainous areas with medium to high seismicity in China. In order to investigate the seismic collapse behavior and risk, a scaled frame model was tested under constant axial load and reversed cyclic lateral load. Test results show that the failure can be induced by the development of story yielding at the first story above the upper ground. The strong column and weak beam mechanism can be well realized at stories below the upper ground. Numerical analysis model was developed and calibrated with the test results. Three pairs of six case study buildings considering various structural configurations were designed and analyzed, showing similar dynamic characteristics between frames on two ground levels and flat ground of each pair. Incremental dynamic analyses (IDA) were then conducted to obtain the seismic collapse fragility curves and collapse margin ratios of nine analysis cases designated based on the case study buildings, considering amplification of earthquake effect and strengthening measures. Analysis results indicate that the seismic collapse safety is mainly determined by the stories above the upper ground. The most probable collapse mechanism may be induced by the story yielding of the bottom story on the upper ground level. The use of tie beam and column strengthening can effectively enhance the seismic collapse safety of frames on two ground levels.

**Keywords:** moment frame; incremental dynamic analysis; collapse; fragility; earthquake; irregularity

## 1. Introduction

Observations from past earthquakes, especially those occurred in developing countries such as China and India, have made it widely accepted that collapse of structural systems is the primary source of casualties and economic losses in earthquake-induced ground motions. Although modern building codes imply a low probability of collapse, building codes are generally implicit on ways to evaluate the collapse risk. The safety against collapse of building structures subjected to extreme earthquake event has become a major concern to researchers and practicing engineers for decades (Villaverde 2007). Owing to the advancements in earthquake risk assessment and performance-based engineering, efforts to rigorously examine the collapse safety of buildings under earthquake ground motions have been made for in depth understanding of fundamental mechanism of collapse and quantitative evaluation of structure collapse risk. Significant progress has been achieved in the quantification of collapse risk of typical structural systems such as moment frames (e.g. Krawinkler *et al.* 2007, Goulet *et al.* 2007, Zareian *et al.* 2007, Kulkarni *et al.* 2008, Liel *et al.* 2009, Haselton *et al.* 2011, Harrington *et al.* 2016) and structural walls (e.g. Krawinkler *et al.* 2007, Lan *et al.* 2015, Mojiri *et al.* 2015,

Siyam *et al.* 2016). However, previous research on structure collapse safety mainly focused on structural systems that are regular and have been included in the building codes. The collapse safety of structures that cannot meet the building code requirements in terms of regularity has rarely been investigated.

In recent years, along with the rapid economic growth of the south western region of China, a large quantity of reinforced concrete (RC) high-rise buildings have been constructed on mountainous terrain with medium to high seismicity. Because of the scarcity of flat land, many high-rise buildings have to be constructed on foundations placed at ground levels with considerable difference in elevation up to multiple stories, as illustrated in Fig. 1. The stories between the lower and upper grounds may be protected from adjacent soil by retaining wall or appropriate excavation. Deviating from the code specifications, the high-rise RC moment frames supported on two ground levels exhibit unique irregularity in geometry and lateral force transfer characteristics. Firstly, compared with the stories above the upper ground, those below the upper ground are weak stories due to the reduction of number of bays, resulting in a vertical irregularity in strength and stiffness. Secondly, during an earthquake event the entire structure is excited on the upper and lower grounds simultaneously. Previous research (Geli *et al.* 1988, Paolucci 2002, Bouckovalas and Papadimitriou 2005, Nguyen and Gatmiri 2007) has indicated that such local topography has a site effect on earthquake ground motion. In order to account for the complex seismic site effect, an

\*Corresponding author, Professor  
E-mail: [yuntianw@cqu.edu.cn](mailto:yuntianw@cqu.edu.cn)

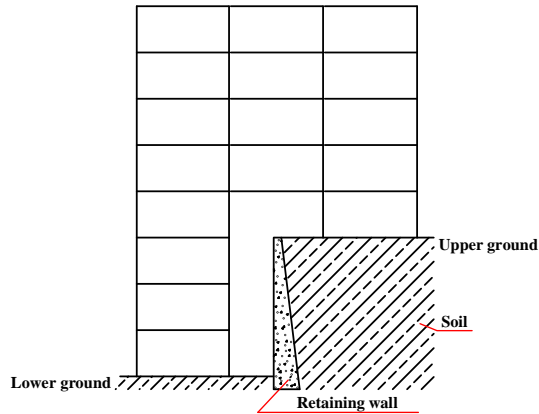


Fig. 1 Moment frame supported on two ground levels

amplification factor is introduced in the Chinese Code for Seismic Design of Buildings (GB 50011-2010). Due to the wide spread of such structures in mountainous regions with medium to high seismicity and lack of research background, it is of great necessity to evaluate the seismic collapse safety of the moment frame structures supported on two ground levels.

In this research program, a 1:4 scaled RC moment frame supported on two ground levels was tested to investigate the failure mode and damage characteristics under simulated earthquake action. Numerical model was then developed and calibrated based on the test results. Three pairs of six two-dimensional RC moment frames were designed as case study buildings in accordance with the Chinese Code for Design of Concrete Structures (GB50010-2010) and GB 50011-2010. Each pair consisted of an irregular frame supported on two ground levels and a regular frame supported on flat ground having the same structural configuration as the portion of the regular frame above the upper ground level. Elastic analyses were carried out on all six frames to compare their fundamental periods and modal shapes. Pushover analysis was conducted to compare their lateral load-displacement characteristics. Then seismic fragility analyses based on incremental dynamic analysis (IDA) were conducted to assess the risk of collapse of nine cases designated based on the case study buildings. The influences of structural configuration, strengthening measures and amplification of earthquake input on the collapse behavior and risk of the frames on two ground levels were discussed.

## 2. Experimental study

### 2.1 Details of specimen

The specimen was a 1:4 scaled five-story and three-bay RC moment frame supported on two foundations. The overall dimensions and member identification are shown in Fig. 2. The two exterior bays were connected to the lower and upper ground levels respectively with two stories below the upper ground level. The height of each story was 750 mm and the bay width was 1500 mm. The cross sections of typical beam and column were 100 mm×150 mm and 150

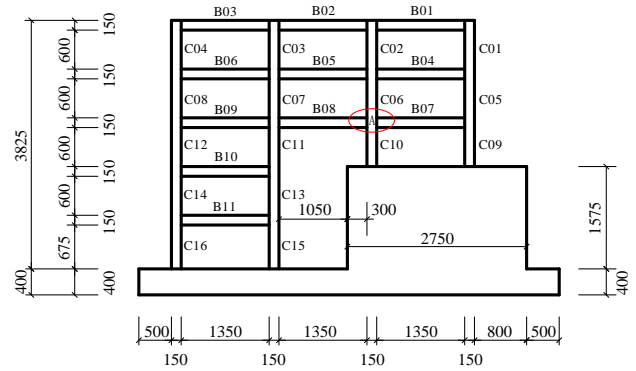


Fig. 2 Overall dimensions of specimen

mm×150 mm respectively. 4 No. 6 (6mm nominal diameter) and 4 No. 8 hot-rolled deformed bars (HRB) with nominal yield strength of 400 MPa were used as longitudinal reinforcing bars for beams and columns respectively. No. 4 HRB rebars with nominal yield strength of 335 MPa were used as transverse reinforcement for beams and columns. The transverse hoops in both beams and columns were spaced by 50 mm and 90 mm for end and middle regions respectively. The average measured compressive strength of concrete was 29.3 MPa.

### 2.2 Test setup and loading protocol

The test setup is depicted in Fig. 3. Axial compression load was applied to each column through vertical hydraulic jacks and approximately maintained constant during testing. Each vertical jack was placed on the spreader beam 1/3 bay width away from the interior column. The resulting axial load on each interior column was twice of that on each exterior column. To simulate the horizontal earthquake action, reversed cyclic lateral loading was applied at the third floor and roof level and during testing. The ratio of lateral displacements at the third floor to roof level was maintained approximately 1:2, which was determined based on modal analysis results. The entire lateral loading process was displacement controlled by roof drift ratio  $\theta_{top}$ , which is defined as the ratio of roof displacement  $\Delta$ , to the structural height  $H_{up}$  measured from upper ground level to the horizontal loading line at roof level. During testing,  $\theta_{top}$  was gradually increased from 0.1% to 5%. Lateral support was provided to restrain the specimen from out-of-plane deformation during testing.

#### 2.3.1 General observations

Concrete cracks were first detected at the left end on the beam B09 corresponding to a lateral displacement of 6.0 mm at the roof. Bottom regions of the columns C09 and C10, which were connected to the upper ground level, started to crack corresponding to the lateral displacement of 9.0 mm at the roof level. Other cracks were mainly developed on beam ends. The bottom region of the column C15, which was connected to the lower ground level, started to crack when the lateral displacement was 14.5 mm. Closely spaced cracks were developed at the top end of column C10. When the lateral roof displacement reached 30



Fig. 4 Deformation of specimen

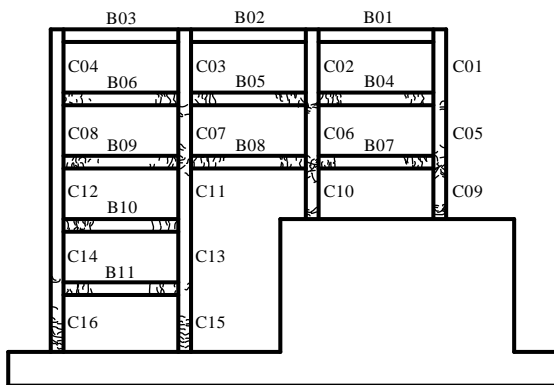


Fig. 5 Distribution of cracks

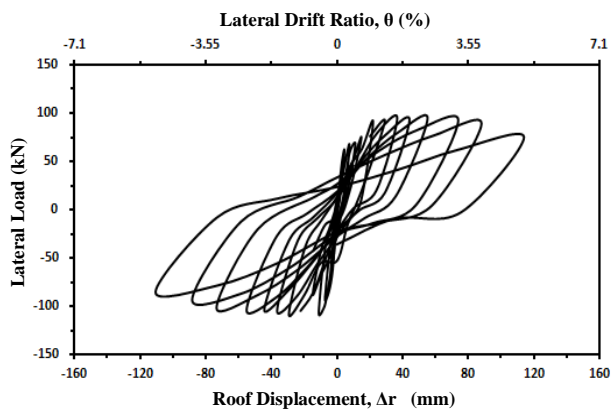


Fig. 6 Measured load-displacement responses

mm, the top and bottom ends of columns C09 and C10 began to spall off and the cracks there were further widened with the increase of lateral displacement. The longitudinal reinforcing bar of the column C09 fractured corresponding to the lateral displacement of 110 mm at the third floor. Significant damages concentrated at joint A. The failure of the specimen was initiated by the formation of bottom story hinge mechanism on the upper ground level, as shown in Fig. 4. Fig. 5 demonstrates the distribution of cracks on members of specimen.

2.3.2 Load-displacement responses

Lateral load-displacement hysteretic curves of the specimen are shown in Fig. 6. Even when the roof lateral displacement reached 110 mm, the lateral load capacity of the specimen didn't drop significantly. The specimen

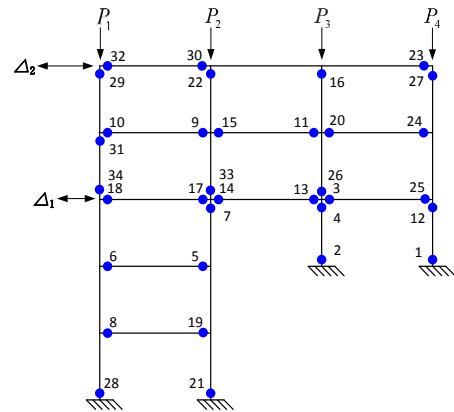


Fig. 7 Yielding sequence of members

exhibited good post-yield deformation capacity and strength retention capacity.

2.3.3 Failure pattern

The failure of the specimen was initiated by the severe concrete crushing and longitudinal rebar fracture of the bottom story columns on the upper ground level. The specimen developed a mixed failure pattern where plastic hinges formed at ends of both beams and several columns. As shown in Fig. 7, the sequence of member yielding was indicated by the numbers. It is clear that the bottom story on the upper ground level exhibited a story yielding mechanism, since the top and bottom ends of the columns yielded. For the stories below the upper ground, however, plastic damages only concentrated at beam ends and the bottom ends of columns of the story right above the lower ground.

2.4 Analytical model

2.4.1 Modeling approach

The finite element (FE) structural analysis program SeismoStruct (2015) was used to perform the analytical simulation. SeismoStruct is capable of predicting the large displacement behavior of moment frames under static or dynamic loading, taking into account both geometric nonlinearities and material inelasticity. A layered fiber approach was used for the nonlinear analysis of the specimen where the beam and column cross-sections were divided into 100 fibers to represent the confined concrete core, unconfined concrete cover and reinforcement. This approach allows prediction of the spread of inelasticity within the member cross section and along the member length. Beams and columns were modeled using force-based inelastic beam-column elements with further discretization into three sub-elements and four integration sections, as shown in Fig. 8. The columns were modeled using a fixed base condition.

The bilinear elasto-plastic material model with kinematic strain-hardening was used for the steel reinforcement. The modulus of elasticity ( $E_s$ ), yield strength ( $f_y$ ), strain hardening parameter ( $\mu$ ) and buckling strain were taken as 200 GPa, 400 MPa, 0.01 and 0.1 respectively. The concrete material was represented by the uniaxial constant

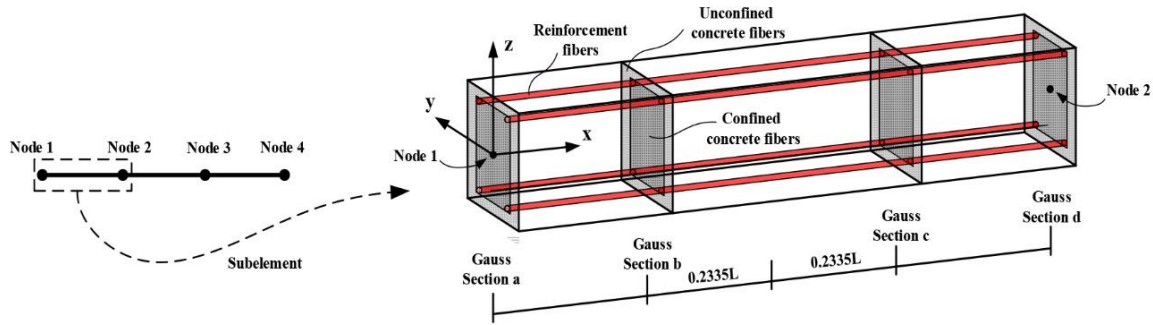


Fig. 8 Force-based beam-column element

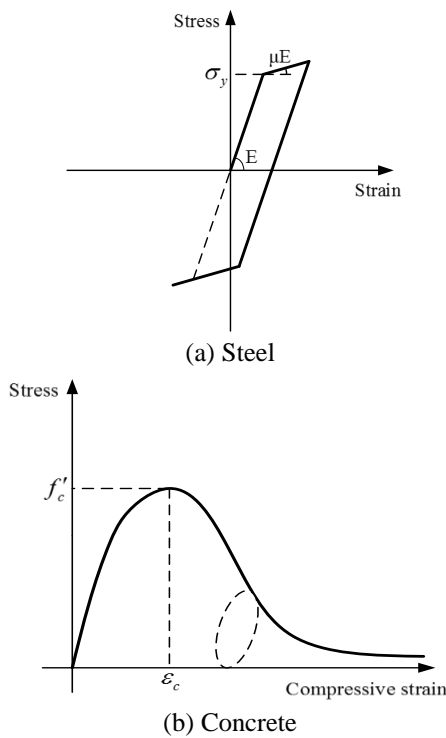


Fig. 9 Material constitutive models

confined model (conc2), as shown in Fig. 9(b). For the conc2 model, four parameters are required: compressive strength  $f'_c$ , tensile strength  $f_t$ , maximum strain  $\epsilon_{co}$  corresponding to  $f'_c$ , and a confinement factor  $k$ . The values of  $f'_c$ ,  $\epsilon_{co}$  and  $k$  are 23.4 MPa, 0.002 and 1.07 respectively.

The confinement effect is taken into account using the model proposed by Mander *et al.* (1988), where the confinement factor  $k$  represents the ratio of the confined concrete compressive strength to the unconfined concrete compressive strength. Ranging from 1.0 to 1.17, the value of  $k$  depends on the transverse and longitudinal reinforcement, concrete strength, and member dimensions and can have a significant effect on the post-yield concrete behavior. The tensile strength of concrete  $f_t$  was ignored herein for better numerical stability.

2.4.2 Analysis results

Comparison between analyzed and experimental results of the total lateral force-top displacement hysteretic curves is shown in Fig. 10. It can be seen that the analysis can

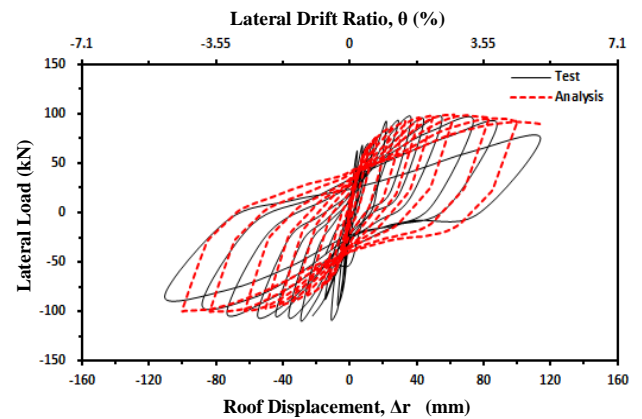


Fig. 10 Measured vs. predicted load-displacement responses

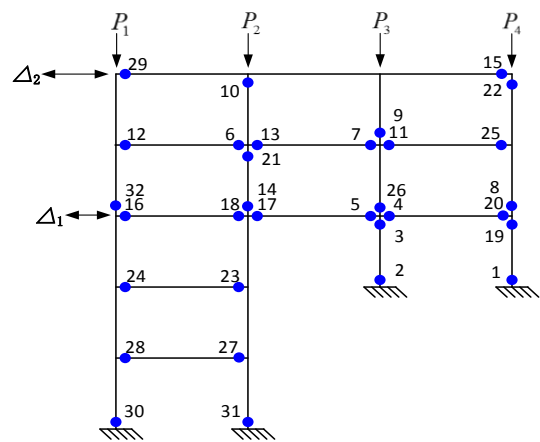


Fig. 11 Analytical yielding sequence

provide a good overall simulation of the experimental results. For the positive loading direction, the simulated curves are in very good agreement with the experimental ones in terms of the strength, stiffness and post-yielding deformation characteristics. For the negative loading direction, the simulation has a greater deviation from the experiment except for the post-yielding stage, resulting in much underestimated stiffness. This deviation was largely due to the fact in the analysis with SeismoStrut, the foundation of the upper stories was assumed rigid while in the experiment it exhibited certain deformability. The simulated yielding sequence is also shown in Fig. 11, which demonstrates a good agreement with the experimental results shown in Fig. 7. Both simulation and experiment

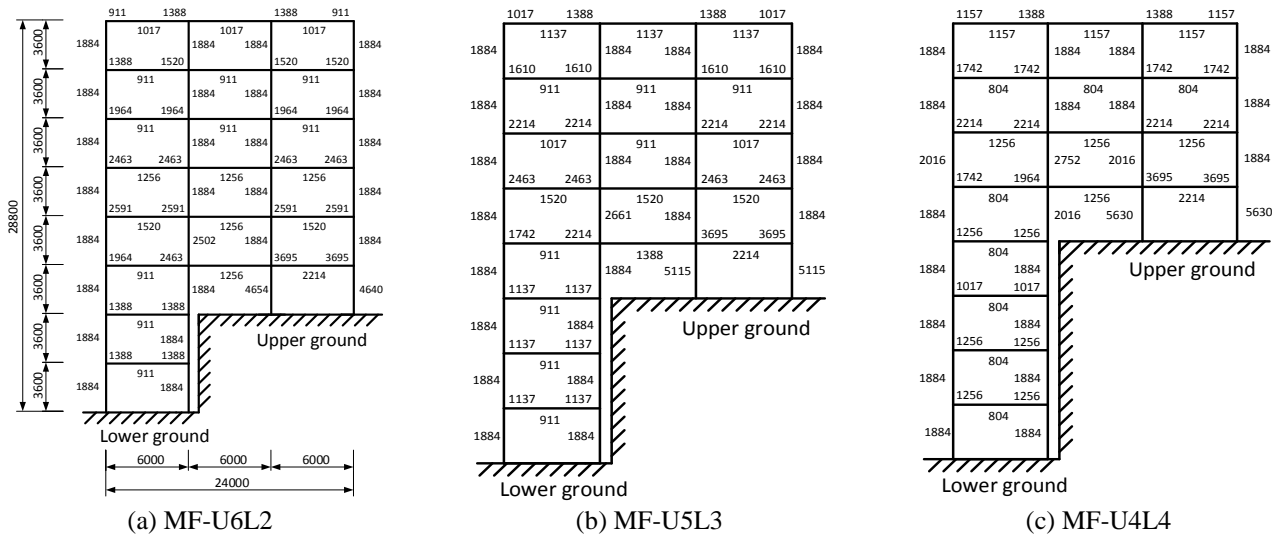


Fig. 12 Longitudinal reinforcement for frame members (unit: mm<sup>2</sup>)

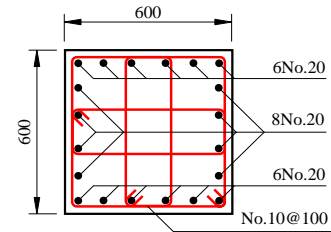
indicate that the bottom story on the upper ground is the weak portion of the structure and develops a story yielding mechanism. The stories below the upper ground level, on the contrary, suffer much less damages and can develop the preferred beam yielding mechanism.

### 3. Case study buildings

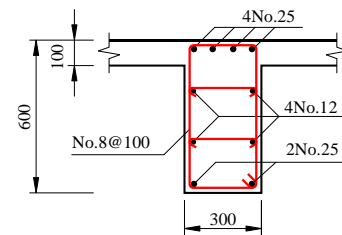
#### 3.1 Building description

In order to further investigate the seismic collapse behavior of irregular high-rise RC moment frames supported on two ground levels, three pairs of six plane moment resisting frames were designed and studied. Each pair consisted of a frame supported on two ground levels and a regular frame supported on one ground level with the same height as that of the other frame above the upper ground level. The frames supported on two ground levels from the three pairs were identified by MF-U6L2, MF-U5L3 and MF-U4L4 respectively, as shown in Figs. 12(a)-(c). The identification of MF-U6L2, for example, indicated six stories above the upper ground level while two stories below the upper ground. The counterpart frames were regular frames supported on flat ground and identified by MF-U6, MF-U5 and MF-U4 respectively. The identification of MF-U6, for example, indicated six stories on the ground level. All the six frames had the same overall dimensions, with 6m bay width and 3.6 m story height.

All six frames were designed based on GB50010-2010 and GB 50011-2010 following the strong column-weak beam mechanism. The design peak ground acceleration (PGA) was 0.2 g. A Class II soil was used, which corresponds to a rock or stiff soil site having an equivalent shear wave velocity of 250-500 m/s and a site soil layer thickness greater than 5 m (GB50011-2010). Earthquake loading was combined with gravity loading  $G+0.5Q$ , where  $G$  denotes permanent actions, including exterior walls, interior light partitions, and superimposed dead load. Exterior walls and interior light partitions are taken as 2.0



(a) A typical column



(b) A typical beam

Fig. 13 A typical column and beam layout of MF-U5

kN/m<sup>2</sup> and 1.0 kN/m<sup>2</sup>, respectively. Superimposed dead load is 0.75 kN/m<sup>2</sup>.  $Q$  is the live load required by the code (2.0 kN/m<sup>2</sup>). The cross-sectional dimensions are 300 mm×600 mm and 600 mm×600 mm for beams and columns respectively. The compressive strength of the concrete in the frame is 23.4 MPa, where the design steel yield strength is 380 MPa and 300 MPa for the longitudinal and hoop reinforcement, respectively. Reinforcement layouts were identical in beams and columns at all story levels. Figs. 13-14 depict the typical details of the frame models.

#### 3.2 Elastic analysis

The dynamic characteristics of the six frames were evaluated and compared by elastic analysis. Table 1 summarizes the fundamental periods of the six frames obtained by Seismostrut and SAP2000 respectively. The two programs yielded very close results with the maximum error of 2.4%. The two frames of each pair had very similar

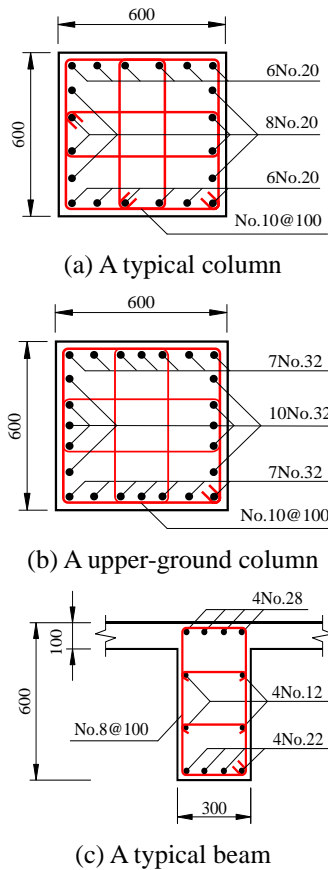


Fig. 14 Column and beam layout of MF-U5L3

Table 1 Fundamental periods of models (sec.)

Analysis Model	Seismostruct	SAP2000	Error (%)
MF-U6L2	0.832	0.852	2.4
MF-U6	0.797	0.799	0.3
MF-U5L3	0.697	0.709	1.7
MF-U5	0.663	0.669	0.9
MF-U4L4	0.567	0.559	1.4
MF-U4	0.531	0.539	1.5

fundamental periods, though the fundamental period of the frame supported on flat ground is greater than that of the one supported on two ground levels up to 5%. For MF-U6L2, MF-U5L3 and MF-U4L4, the fundamental periods are decreased in sequence, which is consistent with the trend among their counterparts, MF-U6, MF-U5 and MF-U4. The normalized modal shapes of the three pairs of frames are shown in Fig. 15. It can also be seen that the frames of each pair have very similar modal shapes. According to the comparison of the elastic analyses of the six frames, it is indicated that the dynamic characteristics of frames supported on two ground levels are mainly dominated by the stories above the upper ground. When the total story number is the same, the higher the portion above ground level, the more flexible the entire structure.

### 3.3 Push-over analysis

The modal push-over analysis (MPA) developed by

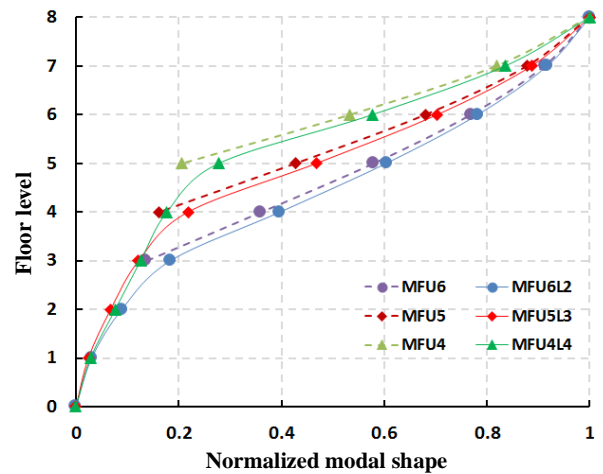


Fig. 15 Modal shapes comparison

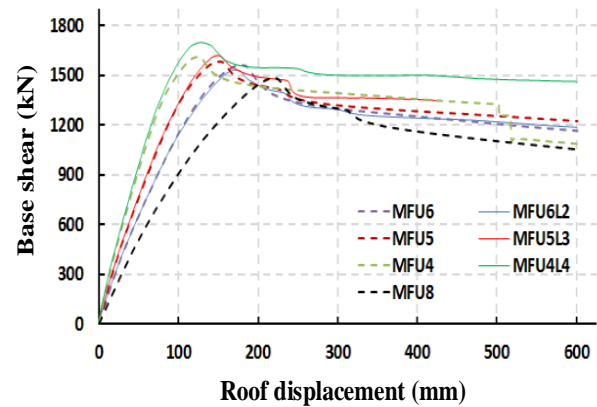


Fig. 16 Push-over analyses results

Chopra and Goel (2001) was carried out to examine the lateral deformation and capacity characteristics through a series of incremental nonlinear static analyses into inelastic range. For the purpose of comparison, three pairs of analysis cases were conducted, i.e., MF-U6L2 and MF-U6, MF-U5L3 and MF-U5, and MF-U4L4 and MF-U4. The push-over analyses results are given in Fig. 16. The ascending and post-yielding segments of the lateral displacement and lateral load curves have very little variation for the three pairs. However, for the pair MF-U4L4 and MF-U4, the push-over curve variation after yielding is noticeable, showing when the structural height below the upper ground is comparative to that above the upper ground the post-yielding lateral behavior can be largely changed. In addition, for each pair of frames, the frame supported on two ground levels exhibits better ductility behavior than the one supported on flat ground.

## 4. Seismic collapse analysis

### 4.1 Methodology

In this study, incremental dynamic analysis (IDA) is adopted to evaluate the seismic collapse safety of RC MFSB. IDA is consisted of a series of nonlinear dynamic

Table 2 22 Far-Field ground motion records

No.	Event	Year	Station	Component	$M^1$	Soil <sup>2</sup>	$E^3$ (km)
1	Northridge, USA	1994	Beverly Hills - Mulhol	NORTHR/MUL279	6.7	D	13.3
2	Northridge, USA	1994	Canyon Country-WLC	NORTHR/LOS270	6.7	D	26.5
3	Duzce, Turkey	1999	Bolu	DUZCE/BOL090	7.1	D	41.3
4	Hector Mine, USA	1999	Hector	HECTOR/HEC090	7.1	C	26.5
5	Imperial Valley, USA	1979	Delta	IMPVALL/H-DLT352	6.5	D	33.7
6	Imperial Valley, USA	1979	El Centro Array #11	IMPVALL/H-E11140	6.5	D	29.4
7	Kobe, Japan	1995	Nishi-Akashi	KOBE/NIS000	6.9	C	8.7
8	Kobe, Japan	1995	Shin-Osaka	KOBE/SHI090	6.9	D	46.0
9	Kocaeli, Turkey	1999	Duzce	KOCAELI/DZC180	7.5	D	98.2
10	Kocaeli, Turkey	1999	Arcelik	KOCAELI/ARC090	7.5	C	53.7
11	Landers, USA	1992	Yermo Fire Station	LANDERS/YER360	7.3	D	86.0
12	Landers, USA	1992	Coolwater	LANDERS/CLW-LN	7.3	D	82.1
13	Loma Prieta, USA	1989	Capitola	LOMAP/CAP000	6.9	D	9.8
14	Loma Prieta, USA	1989	Gilroy Array #3	LOMAP/GO30090	6.9	D	31.4
15	Manjil, Iran	1990	Abbar	MANJIL/ABBAR-T	7.4	C	40.4
16	Superstition Hills, USA	1987	El Centro Imp.Co.	SUPERST/B-ICC090	6.5	D	35.8
17	Superstition Hills, USA	1987	Poe Road(temp)	SUPERST/B-POE360	6.5	D	11.2
18	Cape Mendocino, USA	1992	Rio Dell Overpass	CAPEMEND/RIO360	7.0	D	22.7
19	Chi-Chi, Taiwan	1999	CHI101	CHICHI/CHY101-N	7.6	D	32.0
20	Chi-Chi, Taiwan	1999	TCU045	CHICHI/TCU045-E	7.6	C	77.5
21	San Fernando, USA	1971	LA-Hollywood Stor	SRERNPEL180	6.6	D	39.5
22	Friuli, Italy	1976	Tolmezzo	FRIULI/A-TMZ270	6.5	C	20.2

analyses using a multiply scaled suite of ground motion records (Vamvatsikos and Cornell 2002). A great deal of research has been carried out with IDA to reveal significant dynamic response characteristics of building structures. Zareian and Krawinkler (2007) investigated the effect of uncertainties on the probability of collapse of an 8-story moment-resisting frame. Liao *et al.* (2007) estimated the system capacity against incipient collapse of a spatial steel frame. Haselton *et al.* (2011) evaluated the risk of collapse of thirty archetypical RC special moment frames, ranging in height from 1 to 20 stories, to quantify the seismic safety implied by modern building codes. Brunesi *et al.* (2015) investigated the progressive collapse risk of two building classes representative of European buildings designed for gravity loads and earthquake in accordance with Eurocodes 2 and 8, respectively. In order to reduce the computational cost of the conventional IDA, progressive IDA was developed where the ground motion records are calculated in the precedence list. The case study on a 4-story RC frame structure demonstrated that the progressive IDA can reduce more than 80% computational efforts with only 10% error (Azarbakht and Dolšek 2011).

The following steps were carried out to quantitatively assess the seismic collapse safety of RC MFSB: 1) calibrating nonlinear structural models; 2) compiling an appropriate set of ground motion records; 3) normalizing and scaling ground motion records; 4) selecting suitable intensity and damage measures; 5) running the dynamic analyses; 6) post-processing the data to generate the IDA curves and collapse fragility curves; 7) calculating the collapse margin ratio (CMR) and assessing the seismic collapse safety of each model.

#### 4.2 Input ground motions

FEMA P695 (2009) provides two sets of ground motion records for seismic collapse assessment. The Far-Field record set is suggested for the use of collapse evaluation, while the Near-Field record set is provided as a supplement to examine the near-fault effects on structures. The Far-Field record set includes 22 component pairs of horizontal ground motions from large-magnitude events in the Pacific Earthquake Engineering Research Center (PEER) Next Generation Attenuation (NGA) database (PEER 2006a). In order to consider the variability of ground motion records, no more than two records were taken from the same earthquake. Then 22 ground motion records of the 44 Far-Field records, as listed in Table 2, were adopted as the pre-defined ground motions and scaled to increase intensities until the structures reach the collapse limit.

#### 4.3 Intensity and damage measures

The intensity measure (IM) and the damage measure (DM) are used to indicate the input ground motion intensity and measure the structural response respectively in IDA (Vamvatsikos and Cornell 2002). In this study,  $S_a(T_1, 5\%)$  is selected as the intensity measure. Previous studies have shown that the selection of  $S_a(T_1, 5\%)$  as IM is appropriate for buildings with medium height (hence first-mode-dominated), since the IDA curves exhibited low dispersion, and the magnitude or source-to-site distance information was not necessary for providing a complete characterization of structural response (Shome and Cornell 1999, Vamvatsikos and Cornell 2004). The maximum peak inter-

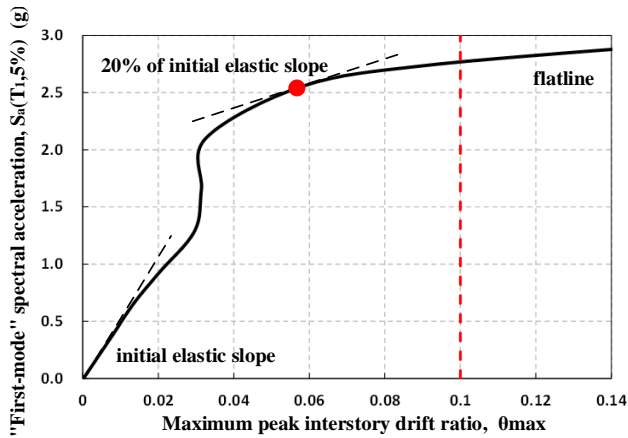


Fig. 17 Definition of collapse

Table 3 Variables and fundamental period of study models

ID	Design frame ID	AF <sup>1</sup>	Strengthening method	Fundamental period $T_1$ (s)
Case-1	MF-U6L2	1.00	—	0.832
Case-2	MF-U5L3	1.00	—	0.697
Case-3	MF-U4L4	1.00	—	0.567
Case-4	MF-U5L3	1.15	—	0.697
Case-5	MF-U5L3	1.30	—	0.697
Case-6	MF-U5L3	1.00	Rigid tie beam <sup>2</sup>	0.673
Case-7	MF-U5L3	1.30	Rigid tie beam <sup>2</sup>	0.673
Case-8	MF-U5L3	1.00	Enlarging column size <sup>3</sup>	0.616
Case-9	MF-U5L3	1.30	Enlarging column size <sup>3</sup>	0.616

<sup>1</sup>amplification factor for upper-ground input ground acceleration

<sup>2</sup>rigid tie beam between upper ground and third floor on lower ground

<sup>3</sup>Enlarging cross section of first and second story columns on upper ground from 600×600 mm to 900×900 mm

story drift ratio  $\theta_{\max}$ , which is the maximum inter-story drift ratios over time and over all stories recorded during the time history analyses, can adequately reflect the global dynamic instability and structural performance limit-states; thus, it is employed herein as the DM.

#### 4.4 Collapse criteria

In this study, sidesway collapse is the major failure mechanism under concern. The collapse prediction is mainly based on excessive lateral deformation and lateral dynamic instability. As shown in Fig. 17, the limit-state of collapse prevention on an IDA curve is defined as the point where the tangent is equal to 20% of the initial elastic slope or the maximum peak inter-story drift ratio  $\theta_{\max}$  reaches 10%, whichever comes first. The main idea is to place the collapse prevention limit-state at a point where the IDA curve is on softening branch with values of  $\theta_{\max}$  low enough so that the structural model can still be trusted. To obtain complete IDA curves, piecewise linear approximation is adopted.

#### 4.5 Analysis cases

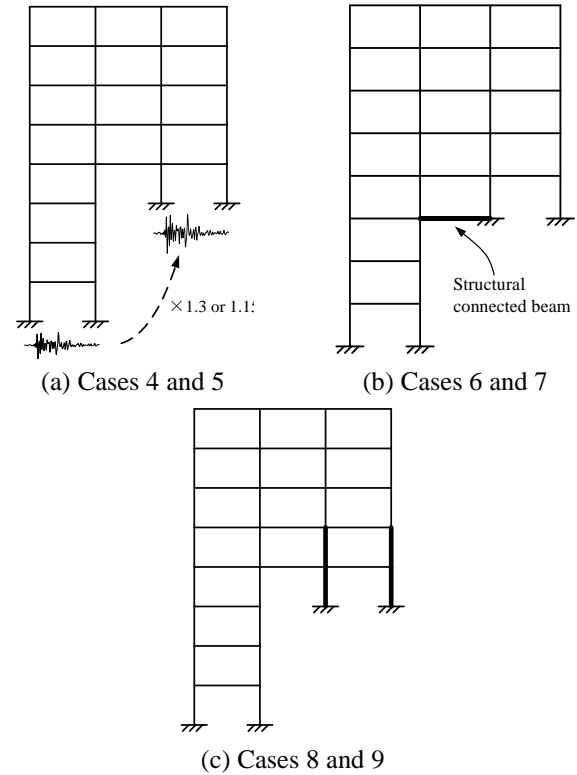


Fig. 18 Analysis cases

Totally nine IDA cases were analyzed with SeismoStruct (2015). Table 3 summarizes the parameters of the nine cases. Cases 1 to 3 were the analyses of the case study buildings MF-U6L2, MF-U5L3 and MF-U4L4 respectively, aiming to examine the influence of the number of stories below the upper ground level on the seismic collapse risk. In cases 4 and 5, MF-U5L3 was analyzed considering the amplification of earthquake input at the upper ground due to the special local topography, as shown in Fig. 18(a). According to GB 50011-2010, the amplification factor is associated with the height of the prominent terrain  $H$ , the ratio of the height  $H$  to horizontal projection length of the slope, and the ratio of the height  $H$  to the distance between structure and slope edge. The amplification factors were 1.15 and 1.3 for case 4 and case 5 respectively. In cases 6 and 7, rigid tie beams were used in the frame MF-U5L3 to connect the upper ground to the third floor on the lower ground level, as depicted in Fig. 18(b). In cases 8 and 9, the first and second story columns on the upper ground in MF-U5L3 were strengthened by enlarging the cross-sectional dimension from 600 mm×600 mm to 900 mm×900 mm without changing the amount of the reinforcing bars. The upper ground earthquake amplification factors for cases 8 and 9 were 1.0 and 1.3 respectively.

## 5. Results of seismic collapse assessment

### 5.1 Seismic fragility curves

Incremental dynamic analysis was conducted for each case using the selected suite of ground motion records and

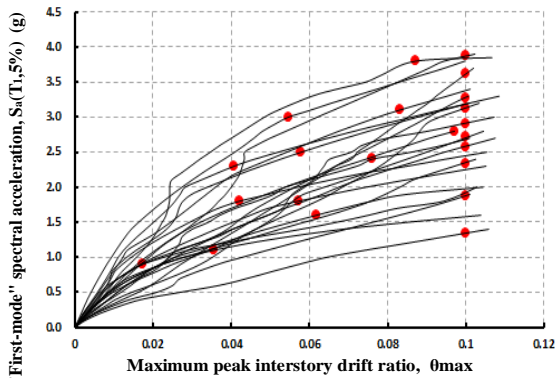


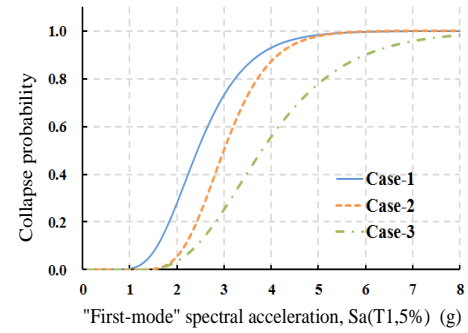
Fig. 19 Multi-record IDA curves of Case 1

multi-record IDA curves were obtained. Fig. 19 shows the 22 IDA curves for Case 1. The solid red marker on each IDA curve indicates the onset of sidesway collapse. The collapse fragility curve can be defined through a cumulative distribution function, which relates the intensity measure to the probability of collapse. A series of comparison between the collapse fragility curves for obtained by fitting a lognormal distribution to the collapse data, as illustrated in Figs. 20(a)-(d).

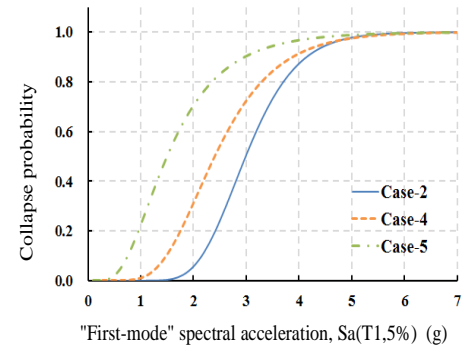
Fig. 20(a) compares the fragility curves for cases 1 to 3, where the variation parameter is the number of stories below the upper ground. The median collapse spectral accelerations of cases 1 to 3 corresponding to 50% collapse probability, or  $S_a(T_1, 50\%)$ , are 2.44, 2.99 and 3.78 respectively. This means that when the total number of stories is constant (eight stories), the increase of number of stories below the upper ground, or the decrease of the number of stories above the upper ground, can benefit the seismic collapse behavior. The adverse impact of amplification factor on seismic collapse behavior can be seen from Fig. 20(b), where the amplification factors for Cases 2, 4 and 5 are 1.0, 1.15 and 1.3. Cases 2, 6 and 8 were designed to examine the effect of various strengthening methods. In all the three cases three stories were below the upper ground. In case 6, a rigid tie beam was used to connect the upper ground and the adjacent bay. In case 8, the first and second story columns above the upper ground level were strengthened by enlarging cross sectional areas. According to Fig. 20(c) the values of  $S_a(T_1, 50\%)$  for cases 2, 6 and 8 are 2.99, 3.36 and 4.0, indicating that both tie beams and column strengthening can improve the seismic collapse behavior. Column strengthening can be more effective than tie beam in improving the seismic collapse behavior. The only difference between Fig. 20(c) and (d) is that an amplification factor of 1.3 is considered. The resulting values of  $S_a(T_1, 50\%)$  for cases 5, 7 and 9 are 1.50, 1.90 and 2.17, showing that the effect of the strengthening measures in improving the seismic collapse behavior can be more noticeable when the earthquake input at the upper ground is amplified.

### 5.2 Collapse margin ratio

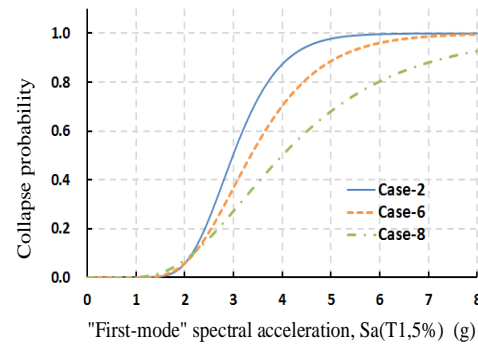
To quantify the collapse possibility of each analysis case, the collapse margin ratio (CMR) was calculated and



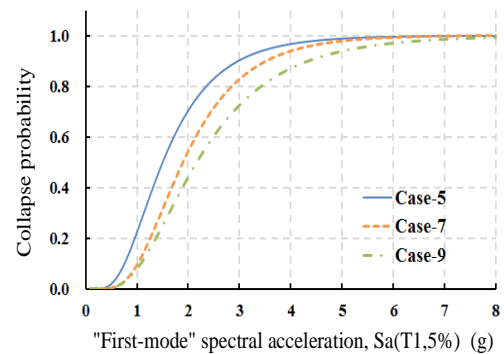
(a) Cases 1 to 3



(b) Cases 2, 4 and 5



(c) Cases 2, 6 and 8



(d) Cases 5, 7 and 9

Fig. 20 Collapse fragility curves

summarized in Table 4. CMR is a primary parameter used to characterize the collapse safety of a structure, which is defined as the ratio of the median 5%-damped spectral acceleration of the collapse level ground motions,  $S_C$  (or the corresponding displacement,  $D_C$ ), to the 5%-damped predicted maximum considered earthquake (MCE) spectral acceleration,  $S_{MCE}$  (or the corresponding displacement,

Table 4 CMR of analysis cases

ID	Median collapse intensity (g)	MCR intensity (g)	CMR
Case-1	2.44	0.52	4.69
Case-2	2.99	0.61	4.90
Case-3	3.78	0.73	5.18
Case-4	2.41	0.61	3.95
Case-5	1.50	0.61	2.46
Case-6	3.36	0.63	5.33
Case-7	1.90	0.63	3.02
Case-8	4.00	0.68	5.88
Case-9	2.17	0.68	3.19

Table 5 Occurrence risk of maximum inter-story drift ratio at onset of collapse (%)

ID	Story level (measured from lower ground level)							
	1 <sup>st</sup>	2 <sup>nd</sup>	3 <sup>rd</sup>	4 <sup>th</sup>	5 <sup>th</sup>	6 <sup>th</sup>	7 <sup>th</sup>	8 <sup>th</sup>
Case-1			81.8	18.2				
Case-2				72.7	27.3			
Case-3					100			
Case-4				95.5	4.6			
Case-5				95.5	4.6			
Case-6					100			
Case-7				72.7	27.3			
Case-8	9.09				4.54	86.4		
Case-9				68.2	13.6	18.2		

$D_{MCE}$ ), in the fundamental period of the structure

$$CMR = \frac{S_C}{S_{MCE}} = \frac{D_C}{D_{MCE}} \quad (1)$$

The CMR of cases 1 to 3 are 4.69, 4.90 and 5.18 respectively, showing that the seismic collapse safety can be increased with the decrease of story number above the upper ground, or the increase of story number below the upper ground. For cases 2, 4 and 5, the CMR are 4.90, 3.95 and 2.46 respectively. The decrease of collapse safety of cases 2, 4 and 5 is due to the amplification of earthquake input at the upper ground. The CMR of cases 2, 6 and 8 are 4.90, 5.33 and 5.88. Both tie beam and column strengthening can be effective in improving the collapse safety. The column strengthening is even more effective than tie beam. The CMR of cases 5, 7 and 9 are 2.46, 3.02 and 3.19, showing that under amplified earthquake input at the upper ground, the strengthening measures can be more considerable.

### 5.3 Story collapse mechanisms

To further investigate the seismic collapse characteristics of frames supported on two ground levels, the occurrence probability of the maximum inter-story drift ratio at onset of collapse is summarized in Table 5, where the story number is counted from the lower ground level and the solid blue lines represent the upper ground level. For cases 1 to 2, the story collapse is most likely to occur at the story immediately above the ground level. For case 3, where the story numbers above and below the upper ground level are the same, the collapse can only take place at the bottom

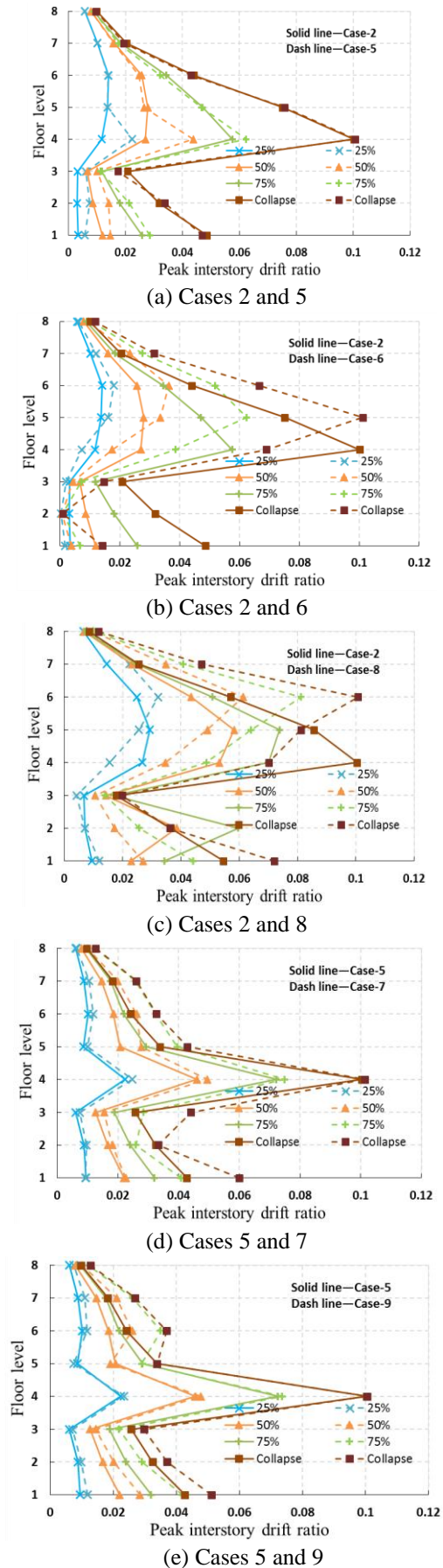


Fig. 21 peak inter-story drift ratio distribution at specified  $S_a(T_i, 5\%)$  levels

story on the upper ground level. For cases 4 and 5, which are similar to case 2 except the earthquake input at the upper ground level is amplified, the probability that collapse occurs at the bottom story above the upper ground level is largely increases. Tie beams are used for cases 6 and 7. The collapse story can be shifted to the second story above the upper ground level, indicating the strengthening effect of tie beam on the bottom story above the upper ground. However, for case 7, the collapse is still more likely to develop at the bottom story above the upper ground, largely due to the amplification effect of earthquake input at the upper ground. For cases 8 and 9, the column enlarging strategy is used to strengthen the two stories above the upper ground. Thus for case 8, the collapse is most likely to occur at the story right above the story strengthened. However, due to the same reason as case 7, the collapse is most probable to happen at the bottom story above the upper ground level.

Figs. 21(a)-(e) depicts the distribution of peak inter-story drift ratios of selected cases along the entire structure height corresponding to 25%, 50%, 75% and 100% of the  $S_a$  ( $T_1$ , 5%) inducing structural collapse. All selected cases are based on case 2, i.e., MF-U5L3, where the 4<sup>th</sup> story measured from the lower ground is the bottom story above the upper ground. The influence of amplification factor is examined in Fig. 21(a). The noticeable distribution variation of peak inter-story drift ratios between case 2 and case 5 is corresponding to the 25% and 50% of the  $S_a$  ( $T_1$ , 5%) inducing structural collapse and mainly occurs at the 4<sup>th</sup> story above the lower ground level, or the 1<sup>st</sup> story above the upper ground. At 75% and 100% of the  $S_a$  ( $T_1$ , 5%) inducing structural collapse, the influence of the earthquake input amplification at the upper ground becomes insignificant. Case 2 and case 6 are compared in Fig. 21(b) to examine the influence of tie beam. It is obvious that the tie beam can enhance the story collapse resistance of the 1<sup>st</sup> story above the upper ground. Thus the peak inter-story drift ratio is shifted to the 2<sup>nd</sup> story above the upper ground level. In Fig. 21(c) case 8 is compared with case 2 to examine the effect of column enlarging method. The little variation between dash lines and solid lines in Fig. 21(d) indicates that under much amplified earthquake input at the upper ground level, the tie beam can yield little improvement in collapse resistance. Similar result is found in Fig. 21(e), where the column enlarging method is used in case 9 with earthquake amplification factor of 1.3. All the figures in Figs. 21(a)-(e) demonstrate that the peak inter-story drift ratio distribution in frame structures supported on two grounds follows similar patterns. The story immediately above the upper ground level suffers the most severe inter-story deformation. The peak inter-story drift ratios gradually decrease upward for the upper stories. However, an abrupt decrease occurs at the story right below the upper ground. Then the peak inter-story drift ratios gradually increase downward for the lower stories.

## 6. Conclusions

In this research program, both experimental and numerical studies have been carried out to investigate the

seismic collapse behavior of moment frames supported on two ground levels, which are widely constructed in mountainous regions with medium to high seismicity in China. The following main conclusions can be drawn. Both the fragility curves and the CMR suggest that compared with the general moment frames in flat terrain, the MF5B exhibited a smaller probability of collapse. And when the sinking stories increase, the collapse probability further reduces. A plausible explanation is given to this by regarding the upper-ground as a “structural wall”.

- According to the experimental results, the failure of the frame supported on two ground levels is caused by the development of story yielding mechanism at the 1st story on the upper ground. At other stories, especially those below the upper ground, the favorite strong column and weak beam mechanism can be well realized.
- The numerical model developed with the program SeismoStrut can simulate the overall behavior of moment frames on two ground levels with adequate accuracy and efficiency. The simulated and experimental results in terms of the lateral load versus lateral displacement relation and the structural member yielding sequence are in good agreement.
- According to the elastic and pushover analyses results, the irregular frame seating on two ground levels has very similar dynamic characteristics such as fundamental period and modal shape to the frame having the same structural configuration above the upper ground. This implies that the stories below the upper ground contribute much less to the overall lateral structural behavior than those above the upper ground level.
- According to the collapse fragility analyses and CMR computation, the seismic collapse safety is mainly determined by the stories above the upper ground. The most probable collapse mechanism may be induced by the story yielding of the bottom story on the upper ground level.
- The tie beam and column strengthening can effectively improve the seismic collapse safety of frames supported on two ground levels. However, the amplification of earthquake excitation at the upper ground can reduce the strengthening effect.

## Acknowledgments

This research project is financially sponsored by Ministry of Science & Technology of China (Grant No. 2016YFC0701302) and the National Science Foundation of China (Grant No. 51578090). The authors would like to express their sincere thanks and appreciation to various supporting agencies of this project.

## References

- Azarbakht, A. and Dolšek, M. (2011), “Progressive incremental dynamic analysis for first-mode dominated structures”, *J. Struct. Eng.*, ASCE, **137**(3), 445-455.
- Bouckovalas, G.D. and Papadimitriou, A.G. (2005), “Numerical

- evaluation of slop topography effects on seismic ground motion”, *Soil Dyn. Earthq. Eng.*, **25**, 547-558.
- Brunesi, E., Nascimbene, R., Parisi, F. and Augenti, N. (2015), “Progressive collapse fragility of reinforced concrete framed structures through incremental dynamic analysis”, *Eng. Struct.*, **104**, 65-79.
- Chopra, A.K. and Goel, R.K. (2001), “A modal pushover analysis procedure for estimating seismic demands for buildings”, *Earthq. Eng. Struct. Dyn.*, **31**, 561-582.
- Federal Emergency Management Agency (FEMA) (2009), Quantification of Building System Performance and Response Parameters (FEMA-P695, ATC-63), Federal Emergency Management Agency, Washington, DC.
- GB 50010 (2010), Code for Design of Concrete Structures, Ministry of Housing and Urban-rural Development, Beijing, China.
- GB 50011 (2010), Code for Seismic Design of Building, Ministry of Housing and Urban-rural Development, Beijing, China.
- Geli, L., Bard, P.Y. and Jullien, B. (1988), “The effect of topography on earthquake ground motion: a review and new results”, *Bull. Seismol. Soc. Am.*, **78**(1), 42-63.
- Goulet, C.A., Haselton, C.B., Mitrani-Reiser, J., Beck, J.L., Deierlein, G.G., Porter, K.A. and Stewart, J.P. (2007), “Evaluation of the seismic performance of a code-conforming reinforced-concrete frame building-from seismic hazard to collapse safety and economic losses”, *Earthq. Eng. Struct. Dyn.*, **36**, 1973-1997.
- Harrington, C.C. and Liel, A.B. (2016), “Collapse assessment of moment frame buildings, considering vertical ground shaking”, *Earthq. Eng. Struct. Dyn.*, **45**, 2475-2493.
- Haselton, C.B., Liel, A.B., Deierlein, G.G., Dean, B.S. and Chou, J.H. (2011), “Seismic collapse safety of reinforced concrete buildings. I: Assessment of ductile moment frames”, *J. Struct. Eng.*, ASCE, **137**(4), 481-491.
- Krawinkler, H. and Zareian, F. (2007), “Prediction of collapse-how realistic and practical is it, and what can we learn from it?”, *Struct. Des. Tall Spec. Build.*, **16**, 633-653.
- Kulkarni, S.A., Li, B. and Yip, W.K. (2008), “Finite element analysis of precast hybrid-steel concrete connections under cyclic loading”, *J. Constr. Steel Res.*, **64**(2), 190-201.
- Lan, W., Ma, J. and Li, B. (2015), “Seismic performance of steel-concrete composite structural walls with internal bracings”, *J. Constr. Steel Res.*, **110**, 76-89.
- Liao, K.W., Wen, Y.K. and Foutch, D.A. (2007), “Evaluation of 3D steel moment frames under earthquake excitations. I: Modeling”, *J. Struct. Eng.*, ASCE, **133**(3), 471-480.
- Liel, A.B., Haselton, C.B., Deierlein, G.G., Dean, B.S. and Baker, J.W. (2009), “Incorporating modeling uncertainties in the assessment of seismic collapse risk of buildings”, *Struct. Saf.*, **31**, 197-211.
- Mander, J.B., Priestly, M.J.N. and Park, R. (1988), “Theoretical stress-strain model for confined concrete”, *J. Struct. Div.*, ASCE, **114**(8), 1804-1826.
- Mojiri, S., El-Dakhkhni, W.W. and Tait, M.J. (2014), “Seismic fragility evaluation of lightly reinforced concrete-block shear walls for probabilistic risk assessment”, *J. Struct. Eng.*, ASCE, **141**(4), 1-13.
- Nguyen, K.V. and Gatzmiri, B. (2007), “Evaluation of seismic ground motion induced by topographic irregularity”, *Soil Dyn. Earthq. Eng.*, **27**, 183-188.
- Paolucci, R. (2002), “Amplification of earthquake ground motion by steep topographic irregularities”, *Earthq. Eng. Struct. Dyn.*, **31**, 1831-1853.
- Seismosoft (2015), SeismoStruct-a Computer Program for Static and Dynamic Nonlinear Analysis of Framed Structures.
- Shome, N. and Cornell, C.A. (1999), “Probabilistic seismic demand analysis of non-linear structures”, Report No. RMS-35, RMS Program, Stanford University, Stanford.
- Siyam, M.A., Konstantinidis, D. and El-Dakhkhni, W. (2016), “Collapse fragility evaluation of ductile reinforced concrete block wall systems for seismic risk assessment”, *J. Perform. Constr. Facil.*, **30**(6), 1-14.
- Vamvatsikos, D. and Cornell, C.A. (2002), “Incremental dynamic analysis”, *Earthq. Eng. Struct. Dyn.*, **31**(3), 491-514.
- Vamvatsikos, D. and Cornell, C.A. (2004), “Applied incremental dynamic analysis”, *Earthq. Spectra*, **20**(2), 523-553.
- Villaverde, R. (2007), “Methods to assess the seismic collapse capacity of building structures. State of the Art”, *J. Struct. Eng.*, ASCE, **133**(1), 57-66.
- Zareian, F. and Krawinkler, H. (2007), “Assessment of probability of collapse and design for collapse safety”, *Earthq. Eng. Struct. Dyn.*, **36**(13), 1901-1914.

CC